Available online at www.sciencedirect.com
SCIENCE DIRECT
International Journal of Hydrogen Energy 31 (2006) 1721–1731
International Journal of HYDROGEN ENERGY
www.elsevier.com/locate/ijhydene

Impacts of external heat transfer enhancements on metal hydride storage tanks

Brendan D. MacDonald*, Andrew M. Rowe

Institute for Integrated Energy Systems, Department of Mechanical Engineering, University of Victoria P.O. Box 3055 STN CSC, Victoria, B.C., Canada V8W 3P6

Available online 21 February 2006

Abstract

The rate at which hydrogen can be drawn from a metal hydride tank is strongly influenced by the rate at which heat can be transferred to the reaction zone. In this work, the impacts of external convection resistance on thermodynamic behaviour inside the metal hydride tank are examined. A one-dimensional resistive analysis and two-dimensional transient model are used to determine the impact of external fins on the ability of a metal hydride tank to deliver hydrogen at a specified flow rate. For the particular metal hydride alloy ($LaNi_5$) and tank geometry studied, it was found that the fins have a large impact on the pressure of the hydrogen gas within the tank when a periodic hydrogen demand is imposed. Model results suggest that the metal hydride alloy at the centre of the tank can be removed to reduce weight and cost, without detrimental effects to the performance of the system.

Keywords: Hydrogen storage; Metal hydrides; Heat transfer; External; Fins; $LaNi_5$

1. Introduction

In recent years there has been increasing interest in using metal hydrides for hydrogen storage due to advantageous characteristics such as low operating pressure, and high volumetric density. One key issue for metal hydride storage systems is limited heat transfer between the fluid on the exterior of the tank and the metal hydride alloy within the tank, where the reaction is taking place. Often, the heat transfer rate is the controlling variable that determines the rate at which hydrogen gas can be extracted from a tank [1]. Augmenting heat transfer rates in metal hydride tanks is important for optimizing the design of hydrogen storage applications.

A number of studies have investigated methods to increase heat transfer rates by manipulating the internal properties of the hydride vessel. This is generally done by attempting to increase the effective thermal conductivity of the hydride bed itself. These methods include but are not limited to: insertion of nickel or aluminum foam [2,3], integration of copper wire net structure [4], compacting metal hydride powder with an expanded graphite [5], and internal heat exchangers [6].

External heat transfer enhancements, such as finned surfaces, are often simple and cheap to manufacture. Because of the ease with which external enhancements can be incorporated onto metal hydride vessels it is important to determine exactly what impact they can have on the overall heat transfer characteristics. For some

* Corresponding author. Tel.: +1 250 7218920; fax: +1 250 7216323.
E-mail address: bdmacdon@uvic.ca (Brendan D. MacDonald).

0360-3199/$30.00
doi:10.1016/j.ijhydene.2006.01.007

Nomenclature

A	area, m^2
C_p	specific heat, J/kgK
E_a	absorption activation energy, J/mol
E_d	desorption activation energy, J/mol
h	heat transfer coefficient, W/m^2K
k	thermal conductivity, W/mK
K	permeability, m^2
L	length of the tank, m
m	hydrogen mass desorbed, kg/m^3s
M	molecular weight, kg/kmol
P	pressure, kPa
r	radius, m
R	universal gas constant, $kPam^3/kmolK$
R_t	thermal resistance, K/W
T	temperature, K
t	time, s
t_w	wall thickness, m
th	fin thickness, m
v	gas velocity (z-direction), m/s
V	gas velocity, m/s

Greek letters

ΔH°	reaction heat of formation, J/kg
ε	porosity
η	efficiency
μ	dynamic viscosity, kg/ms
ρ	density, kg/m^3

Subscripts

0	initial
abs	absorption
b	base (of the tank)
cond	conduction
conv	convection
des	desorption
e	effective
emp	empty
eq	equilibrium
eqa	equilibrium for absorption
eqd	equilibrium for desorption
f	fin
g	gas
H_2	hydrogen
i	interior
mh	metal hydride
s	solid
sat	saturated
si	side (of the tank)
t	top (of the tank)
tot	total
w	wall
∞	external fluid

geometries, the use of external fins may have little impact on performance, but for others it might be quite significant. The objective of this study is to discover what this impact is for a particular tank and alloy, and quantify performance based on the following methods.

First, a one-dimensional thermal analysis is performed on a metal hydride storage cylinder to estimate the relative importance and magnitude of the thermal resistances. This is done for two main cases, with two variations for each. The first case involves a metal hydride tank with no external heat transfer enhancements. The second case involves a metal hydride tank with evenly spaced fins on the exterior. Two variations for each of these cases are also analyzed: (a) the thermal circuit at the beginning of desorption (full tank); and, (b) the situation after two thirds of the hydrogen has been desorbed.

For a more accurate analysis of the system, a numerical model is required which effectively describes the heat and mass transfer, as well as temperature, pressure, and concentration dependent rates of reaction. Several studies have investigated numerical modelling of the conditions in a metal hydride tank [7–11]. Jemni and Nasrallah [7–10] have formulated two-dimensional models describing the behaviour in a metal hydride reactor. They typically treat absorption and desorption separately with two different models. The numerical model being used in this study has adapted their absorption and desorption models and combined them to create a model which can simulate both phenomena simultaneously. Therefore, this model is now capable of simulating dynamic storage applications which inherently involve both absorption and desorption throughout cycling. The system of governing equations is solved using the commercial package FEMLAB®. The model is used to simulate a scenario where the tank is initially full of hydrogen and a pulsed mass flow rate demand is imposed at the tank port. Jiang et al. [12] also employed a pulsed mass flow rate demand. They investigated the behaviour of a metal hydride tank when

it is thermally coupled to a fuel cell system. The simulation was done using a computational environment referred to as the virtual test bed (VTB). Mazumdar et al. [13] investigated the transient nature of metal hydrides, and the effect of external fins. Their study involved a compressor driven metal hydride cooling system, assumed one-dimensional heat conduction, and utilized an explicit finite volume forward in time, central in space (FTCS) scheme to solve the partial differential equations.

This study builds upon the previous work, and utilizes a two-dimensional mathematical model that considers both absorption and desorption simultaneously. This enables more accurate analysis of time-dependent behaviour. Simulations are performed for a cylinder with and without external fins. For a fixed environmental temperature, the comparison between fins and no fins is made by investigating internal hydrogen gas pressure and temperature behaviour throughout the cycles. The finite element method is used to solve the governing partial differential equations.

2. Resistive network analysis

In this work, a single metal hydride storage tank is examined. As shown in Fig. 1, the storage system consists of an aluminum cylinder with a 24 cm length, 2 cm outer radius, and a wall thickness of 3.7 mm. The hydride material inside the tank is assumed to have the properties of $LaNi_5$. Results presented are specific to this geometry and may not apply to tanks with significantly different aspect ratios.

Because the tank has a high aspect ratio, the rate of heat transfer from the environment to the desorption site can be simplified and analyzed as a thermal circuit in the radial direction. Using an equivalent circuit analogy, the rate at which heat is transferred can be determined using,

$$q = \frac{\Delta T}{R_{\mathrm{t,tot}}}, \tag{1}$$

where the thermal resistances for conduction in the radial direction, surface convection, and for finned surfaces are given by the following equations [14]:

$$R_{\mathrm{t,cond}} = \frac{\ln(r_2/r_1)}{2\pi k L}, \tag{2}$$

$$R_{\mathrm{t,conv}} = \frac{1}{h 2\pi r_2 L}, \tag{3}$$

$$R_{\mathrm{fin}} = \left\{ h A_{\mathrm{tot}} \left[1 - \frac{N A_{\mathrm{f}}}{A_{\mathrm{tot}}} (1 - \eta_{\mathrm{f}}) \right] \right\}^{-1}. \tag{4}$$

r_2 and r_1 are the exterior and interior radii respectively, k is the thermal conductivity, L is the height of the tank, h is the convection coefficient, A_{tot} is the total surface area of the tank (including fins), A_{f} is the surface area of a fin, N is the number of fins, η_{f} is the fin efficiency, and ΔT is the temperature difference. The external convection coefficient is assumed to be 150 $\mathrm{W/m^2K}$.

It is important to note that when desorption is driven by an increase in external temperature, the reaction within the tank does not occur evenly throughout the hydride bed. During desorption, the reaction is highly endothermic and can only proceed in locations where there is an adequate heat source. Since, in this case, heat is provided through the exterior walls of the tank, modelling experience has shown that the reaction proceeds like a wave from the exterior to the interior of the tank. This behaviour is important because it creates a phenomenon whereby the thermal resistance of the circuit increases as the reaction proceeds due to the reaction location moving towards the tank centre. Thus, the resistance due to the alloy increases and becomes more significant depending on the state of charge. This phenomenon is illustrated by the model and discussed in more detail in Section 4.

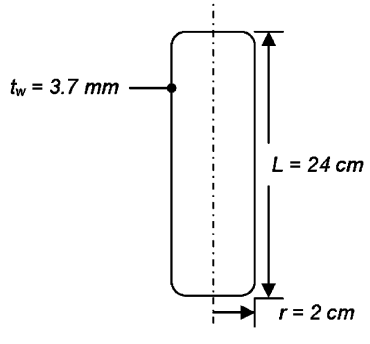

Fig. 1. Schematic of metal hydride tank used in calculations.

2.1. Case 1a: No fins/start of desorption

When the hydride tank is full, and the external temperature is increased, the initial resistance network is shown in Fig. 2a. Heat is driven from the external fluid at T_∞ to the material near the tank wall, at $T_{\mathrm{w,i}}$.

2.2. Case 1b: No fins/desorption two-thirds complete

Once the desorption process has proceeded far enough so that the alloy two-thirds of the distance from

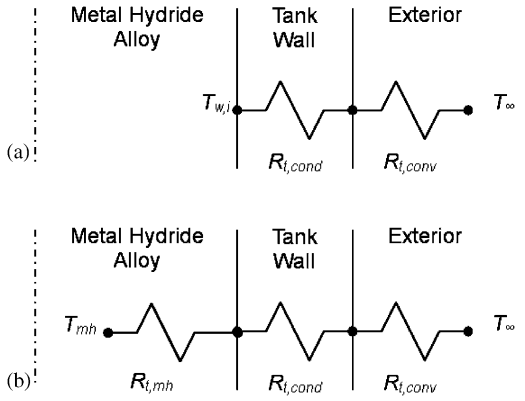

Fig. 2. (a) Schematic of resistance network for Cases 1a and 2a. (b) Schematic of resistance network for Cases 1b and 2b.

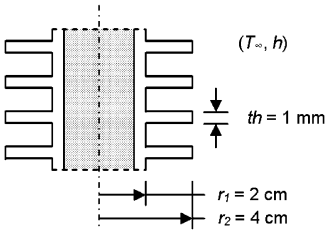

Fig. 3. Cross section of the metal hydride vessel showing the external fin structure used in calculations.

the tank wall has reacted, the resistance network can be drawn as in Fig. 2b. This case assumes that the hydride material near the wall is depleted and that the desorption reaction is occurring near the centre of the tank.

2.3. Case 2a: With fins/start of desorption

For the second case studied, it is assumed that the tank now has a finned structure on the outer radius. The layout and dimensions of the finned tank are shown schematically in Fig. 3. The number of fins on the tank surface is assumed be 50, and the convection coefficient is assumed to be the same as for Case 1.

2.4. Case 2b: With fins/desorption two-thirds complete

The final scenario examined is similar to Case 1b where it is assumed the desorption reaction has proceeded so that only the inner third of the alloy is still charged with hydrogen. The resistance network for this scenario is shown in Fig. 2b. In this case, the external resistance is due to the finned structure. The effective resistance is calculated using Eq. (4).

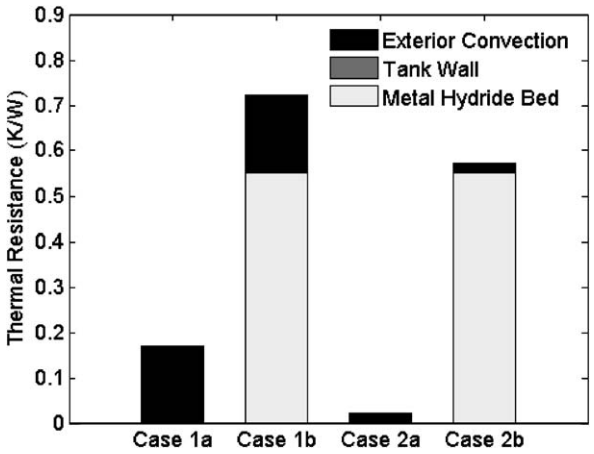

Fig. 4. Results of the thermal circuit analysis.

2.5. Heat transfer results

For the four scenarios described above, the thermal resistances for each component are calculated using the respective geometry, convection coefficient, and material properties. The properties of the hydride are listed in Table 1. The calculated resistances are displayed in Fig. 4. The resistance due to the aluminum tank wall is approximately three orders of magnitude lower than the other resistances and is therefore negligible.

The results in Fig. 4 show that a finned surface decreases the thermal resistance nearly an order of magnitude at the beginning of desorption, whereas, when the reaction has proceeded through two-thirds of the bed, the fins have much less impact on the overall thermal resistance. At this point, the reacted metal hydride alloy has become the dominant resistance.

These results suggest that there is a potential for the external fins to make a significant contribution to the overall heat transfer of the storage system. Therefore, it is reasonable to proceed with a more detailed analysis by using a numerical model. A fully transient simulation will show how the desorption rate changes as the tank is emptied by a pulsed mass flow rate demand.

3. Numerical model

The metal hydride storage system of Fig. 1 is modeled as a two-dimensional axi-symmetric system as shown in Fig. 5. Due to symmetry at the centre of the tank, the governing equations are solved for the r and z directions only. The initial and boundary conditions are labelled in Fig. 5 and listed later in the text. As before, the radius

Table 1
Properties used in the numerical model

Property	Metal ($LaNi_5$)	Hydrogen (H_2)
Saturated density, ρ_{sat} ($kg\,m^{-3}$)	8527	—
Empty density, ρ_{emp} ($kg\,m^{-3}$)	8400	—
Specific heat, C_p ($J\,kg^{-1}\,K^{-1}$)	419	14890
Effective thermal conductivity, k_e ($W\,m^{-1}\,K^{-1}$)	1.32	—
Permeability, K (m^2)	10^{-8}	—
Reaction heat of formation, ΔH° ($J\,kg^{-1}$)	-1.539×10^7	—
Porosity, ε	0.50	—
Molecular weight, M ($kg\,kmol^{-1}$)	—	2.01588
Universal gas constant, R ($J\,mol^{-1}\,K^{-1}$)	—	8.314

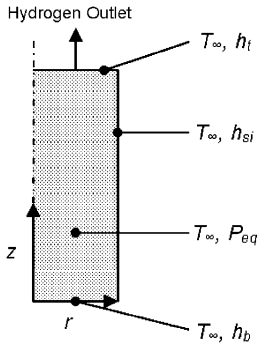

Fig. 5. Schematic of metal hydride tank used in numerical model.

of the tank is 2 cm, and the height is 24 cm. The tank contains the metal hydride alloy $LaNi_5$. The equations governing heat and mass transfer, chemical reaction, and rate of reaction are described in the following.

Assuming thermal equilibrium between the metal hydride alloy and hydrogen gas, a single energy equation can be used. The work of Jemni and Ben Nasrallah [9] supports this assumption for the conditions being examined in this study. They also proved that the advection transport terms can be neglected for this scenario [8]. For a two-dimensional (axi-symmetric) scenario, with r and z axes, the energy equation is

$$(\rho C_p)_e \frac{\partial T}{\partial t} = \frac{1}{r}\frac{\partial}{\partial r}\left(r k_e \frac{\partial T}{\partial r}\right) + \frac{\partial}{\partial z}\left(k_e \frac{\partial T}{\partial z}\right) - m(\Delta H^\circ + T(C_{pg} - C_{ps})), \quad (5)$$

where k_e, C_{pg}, C_{ps}, and m are effective thermal conductivity of the hydride bed, specific heat of the gas and solid phases respectively, and the rate of hydrogen mass absorbed per unit volume. The m term accounts for both absorption and desorption, but as it is used in this study the positive form of m represents absorption, and negative form represents desorption. Adopted from [15] the effective thermal conductivity is assumed to be isotropic and equal to 1.32 W/mK. The $(\rho C_p)_e$ term is the volume averaged heat capacity of the gas and solid and is given below as Eq. (11).

The gas velocity within the reactor can be calculated using Darcy's law

$$V_g = -\frac{K}{\mu_g}\nabla P_g, \quad (6)$$

where K, μ_g, and P_g are the permeability of the porous medium, the dynamic viscosity of hydrogen, and the pressure of the hydrogen gas respectively.

The mass balance expression for hydrogen gas is

$$\varepsilon\frac{\partial(\rho_g)}{\partial t} + \nabla \bullet (\rho_g V_g) = -m, \quad (7)$$

where the m term is the rate of hydrogen mass absorbed per unit volume, as noted above for the energy equation. When solving this equation the hydrogen is assumed to be an ideal gas.

Assuming the solid volume is fixed, the mass balance for the solid is

$$(1-\varepsilon)\frac{\partial(\rho_s)}{\partial t} = m. \quad (8)$$

The expression for the rate of hydrogen absorbed per unit volume is [16]

$$m_{abs} = C_a \exp\left(-\frac{E_a}{R_g T}\right)\ln\left(\frac{P_g}{P_{eqa}}\right)(\rho_{sat} - \rho_s) \quad (9)$$

where C_a is the absorption constant, E_a is the activation energy for absorption, P_{eqa} is the equilibrium pressure for absorption, and ρ_{sat} is the density of the metal hydride alloy when it has absorbed all of the hydrogen gas that can reversibly be absorbed. The equation for the equilibrium pressure is given below as Eq. (14). Adopted from [7], C_a is equal to 59.187 1/s and E_a is equal to 21,179.6 J/mol.

The expression for the amount of hydrogen desorbed per unit time and unit volume is [16]

$$m_{\mathrm{des}} = C_{\mathrm{d}} \exp\left(-\frac{E_{\mathrm{d}}}{R_{\mathrm{g}}T}\right)\left(\frac{P_{\mathrm{g}} - P_{\mathrm{eqd}}}{P_{\mathrm{eqd}}}\right)(\rho_{\mathrm{s}} - \rho_{\mathrm{emp}}), \tag{10}$$

where C_{d} is the desorption constant, E_{d} is the activation energy for desorption, P_{eqd} is the equilibrium pressure for desorption, and ρ_{emp} is the density of the metal hydride alloy when it has desorbed all of the hydrogen gas that can reversibly be desorbed. The equation for the equilibrium pressure is given below as Eq. (14). Adopted from [8], C_{d} is equal to 9.57 1/s and E_{d} is equal to 15,473 J/mol.

These two expressions have been combined in the model by allowing the overall m term to assume the value of either m_{abs} or m_{des}. The logical statements that have been applied to Eqs. (9) and (10) allow for only one of m_{abs} or m_{des} to have a local value other than zero. The m term will assume the value of whichever one is not zero, if both are zero then the m term will also be zero. If m_{des} is used, a negative value is generated since the governing equations are formulated to consider a positive m term as absorption.

This allows the model to simulate absorption and desorption simultaneously, which is essential because within the hydride bed there may be areas that are absorbing hydrogen locally while other areas are desorbing hydrogen. This is especially true of dynamic simulations where there may be rapid variations in hydrogen demands as well as pressure and external temperature.

From the energy equation, Eq. (5), the $(\rho C_{\mathrm{p}})_{\mathrm{e}}$ term is calculated as

$$(\rho C_{\mathrm{p}})_{\mathrm{e}} = (\varepsilon \rho_{\mathrm{g}} C_{\mathrm{pg}} + (1-\varepsilon)\rho_{\mathrm{s}} C_{\mathrm{ps}}), \tag{11}$$

where ε, ρ_{g}, and ρ_{s} are porosity, density of the gas, and density of the solid respectively.

The ideal gas relation used to determine gas density is as follows:

$$\rho_{\mathrm{g}} = \frac{M_{\mathrm{g}} P_{\mathrm{g}}}{R_{\mathrm{g}} T}. \tag{12}$$

The temperature dependent dynamic viscosity term is calculated using [17]

$$\mu_{\mathrm{g}} = 9.05 \times 10^{-6}\left(\frac{T}{293}\right)^{0.68}. \tag{13}$$

The equilibrium pressure for absorption and desorption is calculated using the van't Hoff relationship

$$\ln P_{\mathrm{eq}} = A - \frac{B}{T}, \tag{14}$$

where A and B for P_{eqa} are determined from the Hydride Material Listing Database [18] as $A = 17.608$ and $B = 3704.60$, and A and B for P_{eqd} are determined as $A = 17.478$ and $B = 3704.60$. The different A and B values for P_{eqa} and P_{eqd} are a result of hysteresis. Utilizing different equations for absorption, P_{eqa}, and desorption, P_{eqd}, allows the model to more accurately represent the behaviour within the tank, because hysteresis is accounted for.

3.1. Initial conditions

Initially the pressure, the temperature, and the metal hydride density in the tank are assumed to be constant, the tank is fully charged, and is in a state of equilibrium

$$T(r, z, 0) = T_{\infty}, \tag{15}$$

$$P(r, z, 0) = P_{\mathrm{eqd}}(T_{\infty}), \tag{16}$$

$$\rho_{\mathrm{s}}(r, z, 0) = \rho_{\mathrm{sat}}. \tag{17}$$

The simulation is run for a hydrogen application that does not require hydrogen gas supplied at a high pressure, therefore an ambient temperature of 25 °C (298.15 K) is used as the temperature of the environment (T_{∞}) and no active heat source is required. For the $LaNi_5$ alloy, the equilibrium pressure for desorption (P_{eqd}) that corresponds to this temperature is approximately 156.5 kPa. The tank is initially considered to be full of hydrogen, therefore the density of the solid is the saturated density given in Table 1.

3.2. Boundary conditions

The tank walls are impervious and exchange heat with the environment at constant temperature T_{∞} and a constant heat transfer coefficient, h, of 150 $\mathrm{W/m^2K}$. At the tank outlet (top surface) a periodic mass flow rate demand is imposed as shown in Fig. 6. This represents the hydrogen mass flow rate demand from a fuel cell unit operating at 300 W with an efficiency of 50%. The condition is applied by fixing the velocity of the gas exiting the tank in terms of a constant mass flux divided by the density of the hydrogen gas.

Top surface boundary condition ($z = 24$ cm)

$$k_{\mathrm{e}} \frac{\partial T(r, 24, t)}{\partial z} = h_{\mathrm{t}}(T(r, 0.24, t) - T_{\infty}). \tag{18}$$

Fig. 6 displays the assumed hydrogen flow cycle. Over 15 min intervals the hydrogen demand oscillates between zero and a constant flow of 4.242×10^{-6} kg/s. The duration of the simulation is over four complete cycles and when it ends the storage tank is 78% empty.

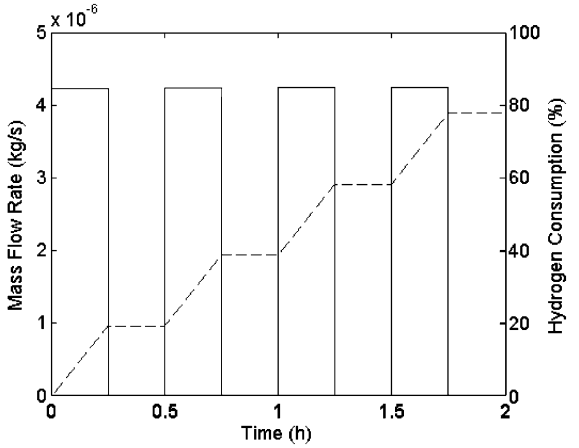

Fig. 6. Hydrogen mass flow rate exiting the tank and cumulative percentage of hydrogen in the metal hydride bed consumed over the two hours of pulsed operation for the simulation with no fins and with fins.

Centre axis boundary conditions ($r = 0\,\text{cm}$)

$$\frac{\partial P(0,z,t)}{\partial r} = 0, \tag{19}$$

$$\frac{\partial T(0,z,t)}{\partial r} = 0. \tag{20}$$

Side surface boundary conditions ($r = 2\,\text{cm}$)

$$\frac{\partial P(0.02,z,t)}{\partial r} = 0, \tag{21}$$

$$k_e \frac{\partial T(0.02,z,t)}{\partial r} = h_{si}(T(0.02,z,t) - T_\infty). \tag{22}$$

Bottom surface boundary conditions ($z = 0\,\text{cm}$)

$$\frac{\partial P(r,0,t)}{\partial z} = 0, \tag{23}$$

$$k \frac{\partial T(r,0,t)}{\partial z} = h_b(T(r,0,t) - T_\infty). \tag{24}$$

The values of the properties used in the model are given in Table 1. These properties are assumed to be constant during the desorption process. For the case with 50 external fins an effective heat transfer coefficient was calculated to be $1177\,\text{W/m}^2\text{K}$. This value is used for h_{si}, to simulate the impact of a finned surface. The thermal mass of the fins themselves is assumed negligible.

The model was implemented using a program called FEMLAB®. When solving partial differential equations, FEMLAB® uses the finite element method. Since the model for the dynamic conditions in a metal hydride canister requires time-dependent partial differential equations, a time-dependent solver is used.

4. Results and discussion

Two simulations were run to simulate the desorption of the tank due to the pulsed hydrogen demand for the case with no fins, and the case with fins. Fig. 6 shows that the hydrogen mass flow rate demand alternates between $4.24 \times 10^{-6}\,\text{kg/s}$ and zero mass flow rate on 15 min intervals. This type of flow demand represents a fuel cell that requires a constant flow rate of hydrogen to maintain a fixed power supply for 15 min and then is shut off for 15 min. In order to maintain a constant flow rate it is assumed that the metal hydride tank is connected to a fuel cell that has a built-in pressure regulator. It can also be seen from Fig. 6 that during the 2 h of pulsed operation the metal hydride storage tank discharges 78% of the total hydrogen initially contained in the tank. This is the same whether the external fins are included or not. The mass flow rate demand is fixed as a boundary condition and therefore it must be the same for both cases. This condition requires that the overall consumption percentage is the same also.

Fig. 7 shows how the density of metal hydride within the tank changes as time proceeds and hydrogen is removed. The plot shows the density of the solid at $z = 12\,\text{cm}$ over the entire time span ($t = 0$–$2\,\text{h}$). As described above, the hydrogen is desorbed in a wave-like manner beginning at the exterior wall, where the heat is provided, and proceeding towards the centre of the tank. This accounts for the majority of the gas desorbed. A secondary desorption is also occurring uniformly throughout the tank during certain time intervals. Along the left edge of Fig. 7, at $r = 0\,\text{cm}$, it can be seen that as time progresses the density at this point decreases. This indicates that a small amount of hydrogen is being desorbed from the centre of the tank, and not just near the edge. Because of the pulsed square-wave nature of the hydrogen demand, there are short periods where desorption is occurring nearly uniformly throughout the bed where the alloy is not locally depleted. When the hydrogen demand is switched on, the hydrogen gas that has built-up within the tank exits and the pressure drops, creating a low enough pressure within the tank to initiate the desorption reaction throughout the regions in the tank that still contain hydrogen. This more uniform reaction exists momentarily until it is restricted by heat transfer limitations (i.e. the temperature decreases locally, causing the equilibrium pressure, which is temperature dependent, to drop). For

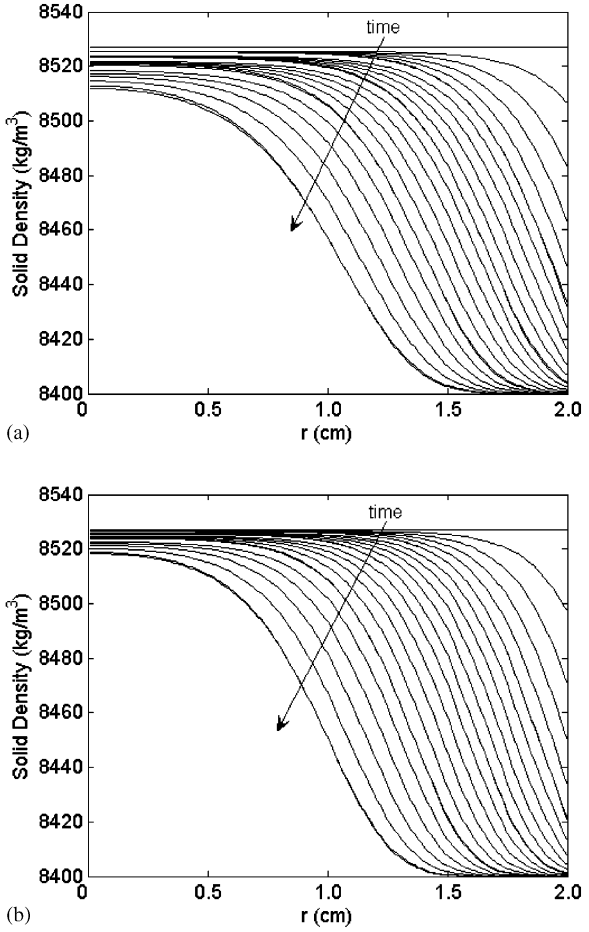

Fig. 7. (a) Density profile of the metal hydride solid for the simulation with no fins at cross section $z = 12$ cm for all times ($t = 0$– 2 h). (b) Density profile of the metal hydride solid for the simulation with fins at cross section $z = 12$ cm for all times ($t = 0$–2 h).

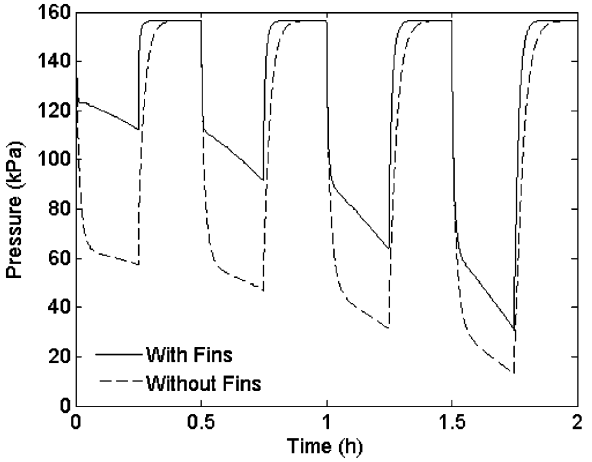

Fig. 8. Hydrogen gas pressure inside the metal hydride tank during the two hours of pulsed operation, showing the comparison between the case with no fins and the case with fins.

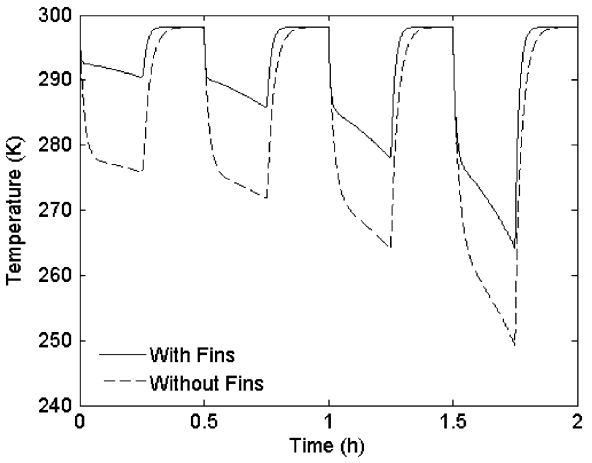

Fig. 9. Temperature at the centre of the tank (at $r = 0$ cm and $z = 12$ cm) during the two hours of pulsed operation, showing the comparison between the case with no fins and the case with fins.

the remainder of a period, the reaction dominates in locations where the thermal wave reaches the reaction zone. The reason for the difference between the amount of hydrogen that is released from the centre region of the tank for the case with no fins in Fig. 7a and the case with fins in Fig. 7b is the faster thermal diffusion near the edge of the tank. Because the fins facilitate heat transfer from the external fluid, the finned case is able to thermally penetrate the reaction zone quicker and prevent the pressure from falling as much, as well as maintain a higher pressure throughout the demand periods as seen in Fig. 8. Thus, the case with no fins reaches a lower pressure than the finned case, and continues to have a lower pressure throughout the demand periods. The endothermic desorption reaction will only proceed if the actual gas pressure is below the equilibrium pressure of the reaction. Since the reaction is endothermic it requires energy to proceed. Therefore, the desorption near the centre of the tank reduces the local temperature, and continues until the equilibrium pressure becomes equal to the gas pressure. For the case with no fins, the gas pressure is lower, therefore the equilibrium pressure reaches a lower value and a much lower temperature is achieved, as seen in Fig. 9. Fig. 9 shows the temperature at the centre of the tank (at $r = 0$ cm and $z = 12$ cm) throughout the two hours of pulsed operation. It can be seen that the temperature drop at the centre of the tank is quite significant during the final hydrogen discharge period, approximately 50 K for the case with no fins and 35 K for the case with fins. However, based on Fig. 7 it can be seen that

the difference between the amount of gas desorbed in the centre region for the case with fins and without is relatively minor.

Throughout the pulsed hydrogen mass flow rate demand there is little spatial variation of the pressure of the hydrogen gas within the tank. The flow of hydrogen is relatively unimpeded by the porous bed and therefore the pressure is able to equalize quickly, even along the z-direction. Thus, the pressure at the centre of the modeled domain (at $r = 1$ cm and $z = 12$ cm) was selected to represent the average pressure of the entire tank. This allows for the comparison of the hydrogen gas pressure within the tank for the case with fins and without as shown in Fig. 8. During hydrogen flow periods the finned case maintains a higher pressure than the case with no fins as noted above. Another difference between the two cases is that during periods of no demand the finned case reaches the equilibrium pressure quicker. As one would expect, as the tank empties, the effect of the fins is reduced. This is illustrated by the difference between the hydrogen gas pressure for the demand periods, the solid line and dashed line in Fig. 8 are progressively coming closer together as time proceeds. This confirms the resistance network analysis results stating that the effect of the fins is reduced as the tank empties. However, in terms of pressure, it should be noted that the fins significantly improve the performance over the majority of the tank's state of fill.

The benefit of this result for hydrogen storage applications is that the tank with external fins can supply hydrogen for a longer period of time given a specific flow demand, and minimum delivery pressure requirement. For example, if the fuel cell system required hydrogen gas at a minimum of 60 kPa, the case with no fins would hardly last for one 15 min discharge period, whereas the case with fins would be able to provide hydrogen above the minimum pressure for three full cycles. This could lead to simpler systems, which require less external heating to provide hydrogen flow.

The temperature within the tank during cycling is not as uniform as the pressure. Fig. 10 shows the large temperature variation in the radial direction at cross section $z = 12$ cm, for the final hydrogen discharge period at times $t = 1.5$–1.75 h. It can be seen that a bulk average temperature value would have little meaning. Fig. 10a shows how the temperature at the outside edge of the tank, $r = 2$ cm, drops well below the temperature of the environment, 298.15 K, for the case with no fins. Conversely, Fig. 10b shows that the tank with fins is able to keep the temperature at the outside edge much closer to the temperature of the environment. Because the finned tank is able to maintain a higher

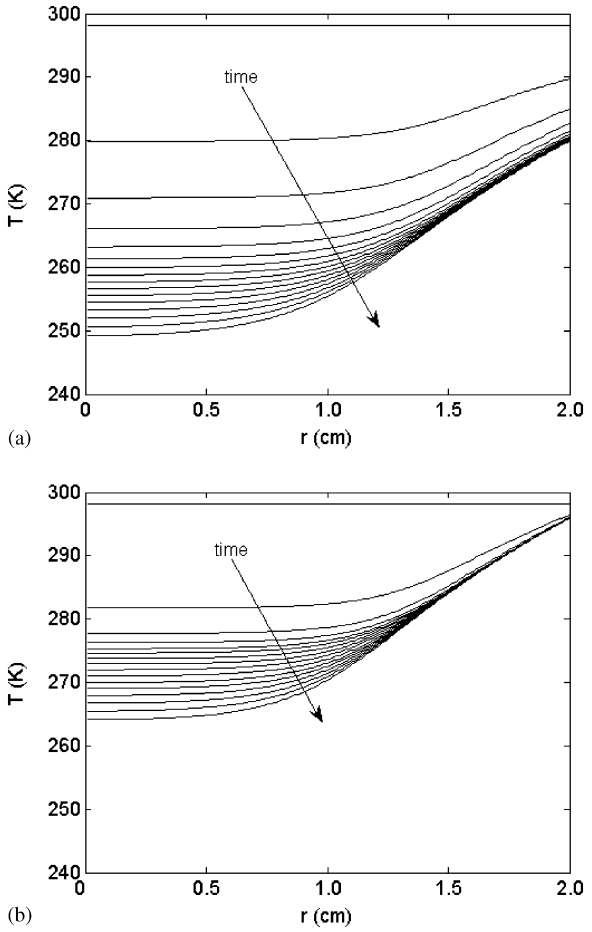

Fig. 10. (a) Temperature profile of the metal hydride bed for the simulation with no fins at cross section $z = 12$ cm for one discharge period at times $t = 1.5$–1.75 h. (b) Temperature profile of the metal hydride bed for the simulation with fins at cross section $z = 12$ cm for one discharge period at times $t = 1.5$–1.75 h.

edge temperature, it also provides increased heat transfer through the hydride bed and the heat is able to reach the reaction zone much quicker. This is consistent with the description given above for Fig. 7, and allows the endothermic desorption reaction to begin releasing hydrogen gas and increasing the pressure within the tank much sooner for the case with fins than the case with no fins. Also of note, is that the temperature at the edge of the tank for the case with no fins remains low even at the end of the demand period.

Fig. 11 illustrates the location along the r-axis where desorption is occurring at cross section $z = 12$ cm, for the final hydrogen discharge period at times $t = 1.5$–1.75 h. Fig. 11a shows a high desorption rate at the centre of the tank during the start of the demand cycle, for the line labelled as $t = 1.5$ h. Fig. 11b shows a much lower

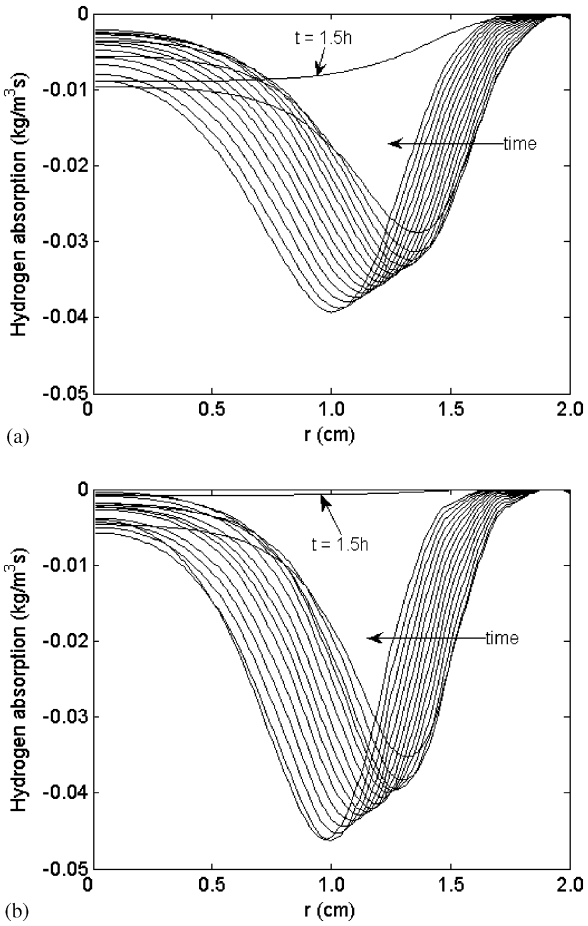

Fig. 11. (a) Profile of the rate of hydrogen mass being desorbed from the metal hydride bed for the simulation with no fins at cross section $z=12$ cm for one discharge period at times $t=1.5$–1.75 h. (b) Profile of the rate of hydrogen mass being desorbed from the metal hydride bed for the simulation with fins at cross section $z=12$ cm for one discharge period at times $t=1.5$–1.75 h.

desorption rate at the centre of the tank. This confirms the phenomenon described above, describing a more uniform desorption throughout the tank at the beginning of each hydrogen flow cycle, and the difference between the case with fins and without. The dip in the curves represents the location of the main reaction zone. The dips at the reaction zone for Fig. 11b reach a lower minimum point and therefore show more concentrated desorption. This is because the temperature in this region is higher, shown in Fig. 10b, and therefore faster desorption occurs.

These results indicate that the addition of external fins can provide a relatively inexpensive but effective way to enhance the performance of a metal hydride storage system that is servicing pulsed hydrogen flow rate demand. The results from these simulations also reveal complex pressure and temperature behaviour that may enable creative solutions to the heat transfer problem. Further dynamic studies into tank behaviour may reveal some interesting methods for enhancing heat transfer to the reaction zone. Another interesting item suggested by this study is the possibility of removing metal hydride alloy from the centre region of the tank. Fig. 7 illustrates that even when the tank is 78% empty, an insignificant amount of hydrogen has desorbed from the centre region. Fig. 8 shows the decreasing performance as the reaction zone approaches the centre of the tank. Therefore the hydride in the centre region is not very effective, and removing it would reduce the weight and cost of the system.

5. Conclusions

The effects of external convection on the thermodynamic behaviour in a metal hydride tank have been studied by resistive analysis calculations, and the use of a numerical model. The preliminary resistive analysis suggested that the addition of external fins on the tank could have a significant impact on the overall heat transfer for the tank geometry and metal hydride alloy used in this study.

This was verified by a numerical model, which found that when the hydrogen is discharged by a pulsed mass flow rate demand, a finned tank is able to maintain a higher supply pressure. The simulations revealed that if the fuel cell system required hydrogen gas at a minimum of 60 kPa, the case with no fins would scarcely last for one 15 min discharge period, whereas the case with fins would be able to provide hydrogen at that pressure for three full cycles. The effect of the fins is also reduced as the tank empties.

This study also revealed some interesting dynamic behaviour for the temperature and desorption rates inside a metal hydride tank. A more detailed investigation into this behaviour could lead to some creative solutions to the heat transfer problem associated with metal hydride storage systems. Another interesting item suggested by this study is the possibility of removing metal hydride alloy from the centre region of the tank. The hydride in the centre region contributes little to fuel delivery, and removing it would reduce the weight and cost of the system.

Acknowledgements

This work was supported by the Natural Sciences and Engineering Research Council of Canada.

References

[1] Sandrock G. A panoramic overview of hydrogen storage alloys from a gas reaction point of view. J Alloys Compd 1999;293–295:877–88.

[2] Chen Y, Sequeira CAC, Chen C, Wang X, Wang Q. Metal hydride beds and hydrogen supply tanks as minitype PEMFC hydrogen sources. Int J Hydrogen Energy 2003;28:329–33.

[3] Lévesque S, Ciureanu M, Roberge R, Motyka T. Hydrogen storage for fuel cell systems with stationary applications—I. Transient measurement technique for packed bed evaluation. Int J Hydrogen Energy 2000;25:1095–105.

[4] Nagel M, Komazaki Y, Suda S. Effective thermal conductivity of a metal hydride bed augmented with a copper wire matrix. J Less-Common Metals 1986;120:35–43.

[5] Klein HP, Groll M. Heat transfer characteristics of expanded graphite matrices in metal hydride beds. Int J Hydrogen Energy 2004;29:1503–11.

[6] Oi T, Maki K, Sakaki Y. Heat transfer characteristics of the metal hydride vessel based on the plate-fin type heat exchanger. J Power Sources 2004;125:52–61.

[7] Jemni A, Ben Nasrallah S. Study of two-dimensional heat and mass transfer during absorption in a metal-hydrogen reactor. Int J Hydrogen Energy 1995;20:43–52.

[8] Jemni A, Ben Nasrallah S. Study of two-dimensional heat and mass transfer during desorption in a metal-hydrogen reactor. Int J Hydrogen Energy 1995;20:881–91.

[9] Ben Nasrallah S, Jemni A. Heat and mass transfer models in metal-hydrogen reactor. Int J Hydrogen Energy 1997;22:67–76.

[10] Jemni A, Ben Nasrallah S, Lamloumi J. Experimental and theoretical study of a metal-hydrogen reactor. Int J Hydrogen Energy 1999;24:631–44.

[11] Mat M, Kaplan Y. Numerical study of hydrogen absorption in an Lm-Ni_5 hydride reactor. Int J Hydrogen Energy 2001;26: 957–63.

[12] Jiang Z, Dougal RA, Liu S, Gadre SA, Ebner AD, Ritter JA. Simulation of a thermally coupled metal-hydride hydrogen storage and fuel cell system. J Power Sources 2005;142: 92–102.

[13] Mazumdar S, Bhattacharyya S, Ramgopal M. Compressor driven metal hydride cooling systems—mathematical model and operating characteristics. Int J Refrig 2005;28:798–809.

[14] Incropera FP, DeWitt DP. Fundamentals of heat and mass transfer. New York: Wiley; 2002.

[15] Askri F, Jemni A, Ben Nasrallah S. Dynamic behaviour of metal-hydrogen reactor during hydriding process. Int J Hydrogen Energy 2004;29:635–47.

[16] Mayer U, Groll M, Supper W. Heat and mass transfer in metal hydride reaction beds: experimental and theoretical results. J Less Common Metals 1987;131:235–44.

[17] White FM. Fluid mechanics. 4th Ed., New York: Mc-Graw Hill; 1999.

[18] Sandrock G, Thomas G. IEA/DOE/SNL Hydride Databases Internet URL http://hydpark.ca.sandia.gov.